Color-Switchable Electroluminescence of Carbon Dot Light-Emitting Diodes

Xiaoyu Zhang,[†] Yu Zhang,[†,‡,§,*] Yu Wang,[‡] Sergii Kalytchuk,[‡] Stephen V. Kershaw,[‡] Yinghui Wang,[§] Peng Wang,[†] Tieqiang Zhang,[§] Yi Zhao,[†] Hanzhuang Zhang,[§] Tian Cui,[§] Yiding Wang,[†] Jun Zhao,[⊥,∥] William W. Yu,[†,⊥,∥,*] and Andrey L. Rogach[‡,*]

[†]State Key Laboratory on Integrated Optoelectronics and College of Electronic Science and Engineering, Jilin University, Changchun, Jilin 130012, China, [‡]Department of Physics and Materials Science and Centre for Functional Photonics, City University of Hong Kong, Kowloon, Hong Kong SAR, [§]State Key Laboratory of Superhard Materials and College of Physics, Jilin University, Changchun, Jilin 130012, China, [⊥]College of Material Science and Engineering, Qingdao University of Science and Technology, Qingdao, Shandong 266042, China, and [∥]Department of Chemistry and Physics, Louisiana State University, Shreveport, Louisiana 71115, United States

ABSTRACT Carbon-dot based light-emitting diodes (LEDs) with driving current controlled color change are reported. These devices consist of a carbon-dot emissive layer sandwiched between an organic hole transport layer and an organic or inorganic electron transport layer fabricated by a solution-based process. By tuning the device structure and the injecting current density (by changing the applied voltage), we can obtain multicolor emission of blue, cyan, magenta, and white from the same carbon dots. Such a switchable EL behavior with white emission has not been observed thus far in single emitting layer structured nanomaterial LEDs. This interesting current density-dependent emission is useful for the development of colorful LEDs. The pure blue and white emissions are obtained by tuning the electron transport layer materials and the thickness of electrode.

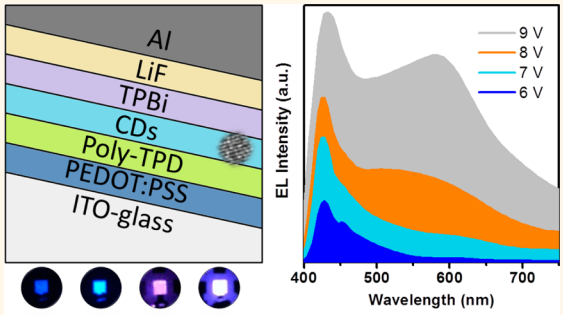

KEYWORDS: carbon dots · color switchable · voltage-dependent · light emitting diode · current density

Solution-processing technology has recently been widely employed to fabricate light-emitting diodes (LEDs). It offers great prospects for developing low-cost, efficient, bright, and large area color displays compatible with flexible substrates.[1−7] Many solution-based nanomaterials have been widely studied and are considered as promising emitting materials.[8−14] The development of high quality quantum dots (QDs) synthesis has stimulated studies on QD-LEDs that exhibit tunable and saturated colors with a narrow emission bandwidth.[15−20] The band-edge electroluminescence (EL) of cadmium-based QDs, *i.e.*, CdX (X = S, Se, Te), exhibits size tunable spectral emission from 450 to 760 nm, allowing for the design and fabrication of color-saturated red, green and blue (RGB) QD-LEDs with simple device configurations for individual pixel based color elements. The high spectral purities of such emitters are becoming comparable with those of liquid crystal displays and organic LEDs.[21−23] With mercury and lead salts based QDs (*e.g.*, HgTe, PbS, and PbSe), the emission from the QD-LEDs has been further extended to the near-infrared regime of 800−2500 nm for a number of nondisplay applications.[24−29]

However, promising as the solution-processed nanomaterials based LEDs are, a serious drawback of the present colloidal QD-LED technology is its dependence on the QDs with toxic heavy-metal components, such as cadmium, lead, and mercury which could potentially hinder their commercialization.[30,31] Since the first synthesis of carbon dots (CDs) reported by Sun *et al.* in 2006,[32] these emerging light-emitting, quantum-sized fluorophores combine several merits of traditional semiconductor-based QDs (such as tunable luminescence emission and high resistance to photo bleaching) without incurring the burden of intrinsic toxicity or elemental scarcity.[33,34] In recent years, CDs have been demonstrated to possess high emission quantum yields (QY, up to 60−80%), which makes them competitive in light-emitting performance

* Address correspondence to yuzhang@jlu.edu.cn, wyu6000@gmail.com, andrey.rogach@cityu.edu.hk.

Received for review September 26, 2013 and accepted November 13, 2013.

Published online November 18, 2013
10.1021/nn405017q

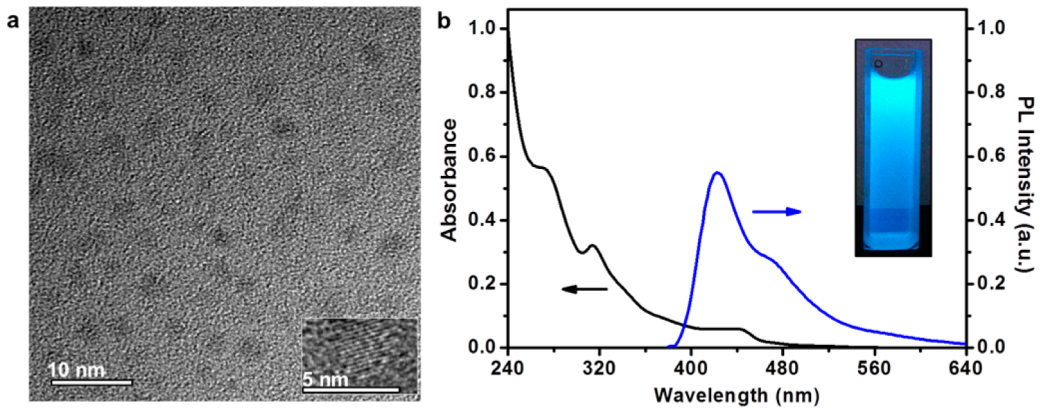

Figure 1. (a) TEM image of CDs, with an inset showing HRTEM image of a single dot; (b) UV−vis absorption and photoluminescence (PL) (340 nm excitation wavelength) spectra of a CD thin film spin-coated on quartz glass, with an inset showing the true-color photograph of CD emission in colloidal solution.

to commercially available core−shell CdSe/ZnS QDs.[35−37] CDs have also been demonstrated to be good electron donors, as well as electron acceptors.[38−40] A series of reports have shown that the efficient and excitation-dependent photoluminescence (PL) of CDs is promising in the fabrication of LEDs and applications for display and solid state lighting.[37,41,42]

In this paper, for the first time we report the observation of multicolor EL from CDs of the same size. Bright blue, cyan, magenta, and white EL emissions were observed from the CD-LEDs with the same CD particles of 3.3 nm. Such a switchable EL behavior with white emission has not previously been observed in single nanomaterial emitting layer structured LEDs, though several nanomaterials have shown the tunability of the EL emission on a single type of emitter.[43−45] The current density-dependent color emission of this type of device is useful for the development of color LEDs and so we investigated several different device structures to optimize its color-tunability which is very important for display applications. The onset voltages, luminance output uniformity, and efficiencies of the CD-LEDs were characterized. The recorded maximum brightness of the devices was 24 cd/m^2 for blue emission and 90 cd/m^2 for white emission, which are the highest values of brightness reported to date compared to the brightness of 35 cd/m^2 from a white light CD-LED made by Wang *et al.*[46] Carrier recombination in the CDs was investigated with time-resolved photoluminescence (TRPL), revealing three typical PL lifetimes. This study is helpful to understand the carrier recombination mechanisms of CDs which are still debated in literature and will facilitate the development of environmentally safe CD-LEDs toward their practical application in next-generation color displays and solid state lighting.

RESULTS AND DISCUSSION

CD-LED Device with Driving Current Controlled Color. A high resolution transmission electron microscopy (HRTEM) image of the carbon dots is shown in Figure 1a. The CDs had an average diameter of 3.3 nm. The absorption spectrum of a CD film and the PL spectrum of the CD solution in toluene at an excitation wavelength of 340 nm are presented in Figure 1b, which exhibit three absorption peaks at 270, 315, and 450 nm, and a main PL peak at 420 nm, respectively. The full width at half-maximum (fwhm) bandwidth of the luminescence band was between 90 and 95 nm, while the PL QY was determined to be ~40%, by using a spectrometer with an integrating sphere and a back-thinned CCD detector.

A schematic of the blue-white CD-LED device structure used in this study is shown in the inset of Figure 2a. The device consists of a patterned ITO anode, a 25-nm thick poly(ethylenedioxythiophene):polystyrene sulfonate (PEDOT:PSS) hole injection layer, a 40-nm poly(*N*,*N*′-bis(4-butylphenyl)-*N*,*N*′-bis(phenyl) benzidine) (poly-TPD) hole transport layer (HTL), a 20-nm CD the emissive layer, a 5-nm 1,3,5-tris(*N*-phenylbenzimidazol-2-yl) benzene (TPBI) electron transport layer (ETL), and a 1-nm LiF and 150-nm aluminum double layer as the cathode. PEDOT:PSS was used as a buffer layer on the anode mainly to increase the anode work function from 4.7 (ITO) to 5.0 eV and to reduce the surface roughness of the anode to obtain stable and pinhole-free electrical conduction across the device.[47] Poly-TPD was used as the HTL in consideration of the fact that its highest occupied molecular orbital (HOMO) level is 5.2 eV which is very close to the work function of the ITO/PEDOT:PSS anode, and also because it possesses an excellent hole-transport capability.[48] Moreover, poly-TPD has been found to have good solubility in organic solvents such as chlorobenzene and thus makes it easy to form a uniform thin layer.[49] TPBI was chosen as the ETL because of its good electron-transport capability and its interfacial phase compatibility with the CD layer.

Figure 2a shows the typical current density and luminance curves as a function of applied voltage for

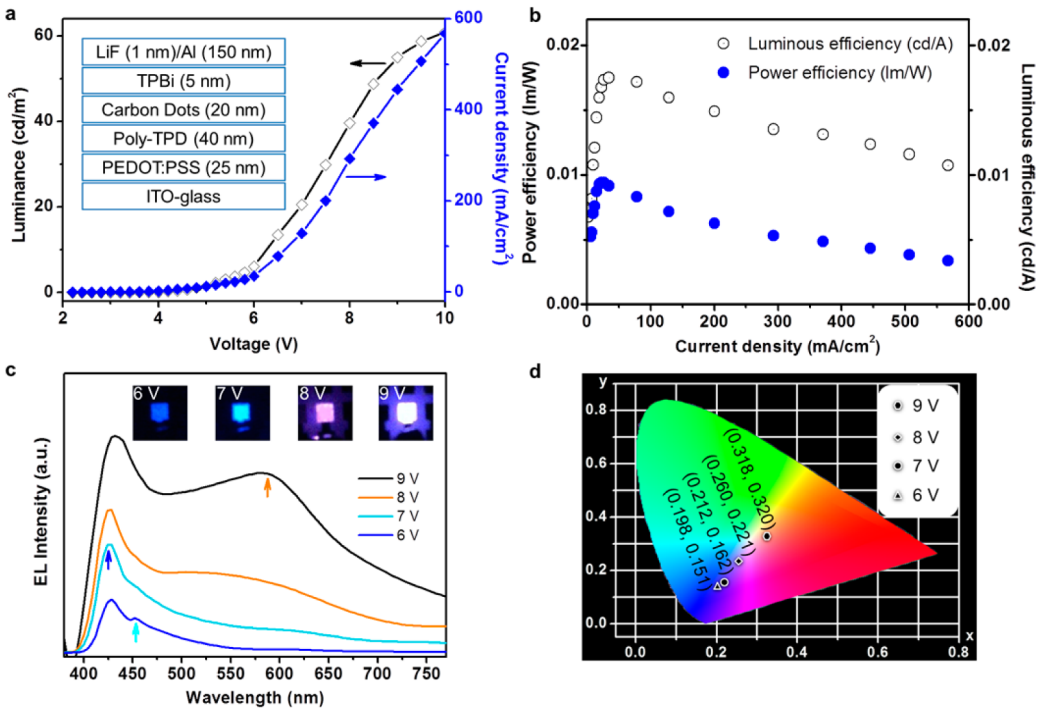

Figure 2. (a) Current density and brightness of the CD-LEDs emitting blue, cyan, magenta, and white light, with an inset showing the device structure comprising ITO/PEDOT:PSS (anode), poly-TPD (HTL), CDs (active layer), TPBi (ETL), and LiF/Al (cathode); (b) the luminous and power efficiencies *vs* current density; (c) electroluminescence (EL) spectra and true color photographs of blue, cyan, magenta, and white emissions; (d) CIE1931 coordinates of the blue, cyan, magenta, and white emission from the same CD-LEDs operated under different voltages.

the CD-LEDs. The variation of the EL efficiency, across the entire measured luminance range and bias, is shown in Figure 2b. The devices demonstrated a low turn-on voltage of 5 V, confirming the reduced barrier height for charge injection into the CD-LEDs. The highest luminance and luminous efficiency reached 61 cd/m^2 and 0.018 cd/A, respectively. The EL spectra of the CD-LEDs, operated at different voltages, are shown in Figure 2c; images of the CD-LEDs under operation are presented in the insets of the figure. The CD-LEDs exhibited bright, uniform and defect-free EL emission over a surface area of 2 mm $\times$ 2 mm. There is no obvious contribution from the polymer HTL or organic ETL in the EL spectra while the similar EL spectra can be obtained from the LED device without the polymer HTL or organic ETL. The Commission Internationale de l'Enclairage (CIE) coordinates of the emitted lights of the CD-LEDs are (0.198, 0.151), (0.212, 0.162), (0.260, 0.221), and (0.318, 0.320) as shown in Figure 2d, corresponding to blue, cyan, magenta, and white lights, respectively. The current−voltage-luminescence and EL spectra could be achieved repeatably for sealed CD-LEDs. The device performance of unsealed CD-LEDs would degrade after the measurement mainly because of the oxidation of the organic layers and the Al electrode.

The light color from the CD-LEDs is apparently voltage-dependent for the same 3.3 nm CD particles (Figure 2c). The blue emission peak at 426 nm in Figure 2c could be observed at a low bias of 6 V. With the increase of bias, the emission peak at 452 nm became stronger, and the color became cyan at the bias of 7 V. With the further increase of bias, the emission at 588 nm appeared and became stronger changing the emission hue to magenta, and finally at higher driving voltage gave white emission from the CD-LEDs. It can be observed that there are three main emissions, peaked at 426, 452, and 588 nm in the white EL spectra, appeared successively with increased bias (Figure 2c). Thus, the white emission at high bias was probably due to the appearance of multiple-recombination processes at high current density. This phenomenon is probably a result of the fact that several recombination mechanisms with different but not too dissimilar (final) excited state lifetimes coexist in each single CD, allowing several recombination pathways without any particular one dominating completely.

The excitation-dependent PL spectra and PL decay curves were recorded in order to understand the recombination processes in the CDs and hence to further control the device emission. Figure 3a shows the evolution of the PL emission spectra of the CDs, which exhibited excitation-dependent emission ranging from 400 to 700 nm, similar to the previous reports.[50−52] When the CDs were excited by a short-wavelength light of 340 nm, a blue emission peaked at 420 nm was observed. When the excitation

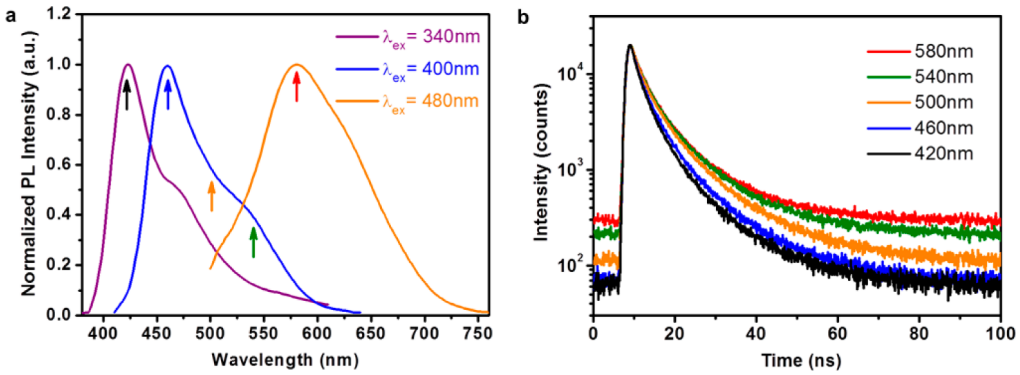

Figure 3. (a) PL spectra of CDs excited by 3 different excitation wavelengths; the color-coded arrows represent the detection wavelength for the PL decay curves in part b; (b) PL decay curves of CDs under 320 nm excitation detected at different wavelengths.

wavelength was 400 nm, the emission peak shifted to 460 nm, the emission at 420 nm became relatively weaker while a small emission peak at 580 nm appeared. With a longer exciting wavelength of 480 nm, the emission peak at 580 nm became stronger. These three peaks were consistent to those observed in the EL spectra of CD-LEDs.

The absorption spectrum of the CD films exhibits three peaks at 270, 315, and 450 nm as shown in Figure 1b. According to previous studies,[53−56] the peak at 270 nm could be ascribed to a $\pi-\pi^*$ transition of aromatic C═C bonds, while the peak at 315 nm may be attributed to an $n-\pi^*$ transition of C═O bonds and the broad peak at 450 nm may originate from the amino-functionalized surface of the CDs. After the excitation wavelength changes from 340 to 400 nm, the strong emission peaked at 420 nm disappears probably because the excitation energy is not sufficient to drive the $\pi-\pi^*$ transition. When the excitation wavelength changes to 480 nm, only the amino group-related emission peaked at 588 nm can be observed. That means that each of the three emission processes of the CDs relies on the excitation and can be selectively controlled *via* the absorption energy. It has to be noted that this phenomenon is quite similar to the recent reported PL from graphene dots, which also exhibits such selectable property attributed to independent molecule-like states through femtosecond transient absorption spectroscopy and femtosecond time-resolved fluorescence dynamics investigation.[57]

PL decay curves have been analyzed in order to further characterize the origin of the emission components of the PL in CDs (Figure 3b). The radiative lifetime of PL emission is an important characteristic of light-emitting nanoparticles.[58,59] Different radiative lifetimes may correspond to different electron−hole recombination mechanisms. Time-resolved, pulsed laser excitation techniques are most suitable for probing the lifetime of PL emission. Figure 3b shows the representative PL decay curves of the CDs, which were probed at different emission wavelengths. The decay fitting

TABLE 1. Fitted decay times and normalized amplitudes of the PL emission of CD film at different wavelengths under 320 nm Excitation

Ex/nm	Em/nm	τ_1/ns	A_1/%	τ_2/ns	A_2/%	τ_3/ns	A_3/%
320	580	2.1	19.1	5.5	47.6	14.0	33.3
	540	2.1	19.6	5.8	49.4	15.0	31.0
	500	2.0	21.1	5.8	49.9	15.1	29.0
	460	2.0	28.4	5.4	49.5	14.8	22.1
	420	2.0	32.4	5.1	48.3	14.0	19.3

results are listed in Table 1, with radiative lifetime τ_1 of 2 ns, τ_2 of 5 to 6 ns, and τ_3 of 14 to 15 ns. It was found that the PL decays of the CDs were emission wavelength dependent. The amplitudes A_1 and A_2 with radiative lifetime of τ_1 and τ_2 account for a large amount of the PL emission spectra at short wavelength. The proportion of amplitude A_1 decreases and the strength of the processes associated with A_3 increases as the emission wavelength shifts from 420 to 580 nm while A_2 does not vary that much. Therefore, the short lifetime of 2 ns can be attributed to the emission peaked at 420 nm, the medium one of 5−6 ns corresponds to the emission peaked at 460 nm, and the long lifetime of 14−15 ns can be attributed to the emission peaked at 580 nm. Normally, relaxations (prior to radiative relaxation) involving the emission of high energy phonons will be more rapid (and so are associated with the fastest decay energy level). Therefore, when the excitation energy is high (*e.g.*, 340 nm), the emission peaked at 420 nm is the dominant recombination channel as shown in Figure 3a. Correspondingly, for the CD-LED's EL emission, when the injection current density is low, the carriers preferentially relax *via* the energy level associated with the faster decay channel. Thus, blue emission was seen at low current density. When the current density was high enough, other emission colors (associated with slower recombination rates) were observed in the CD-LEDs. Therefore, the CD-LED's color-switchable EL is actually driven by the injection current density, not the apparent applied voltage.

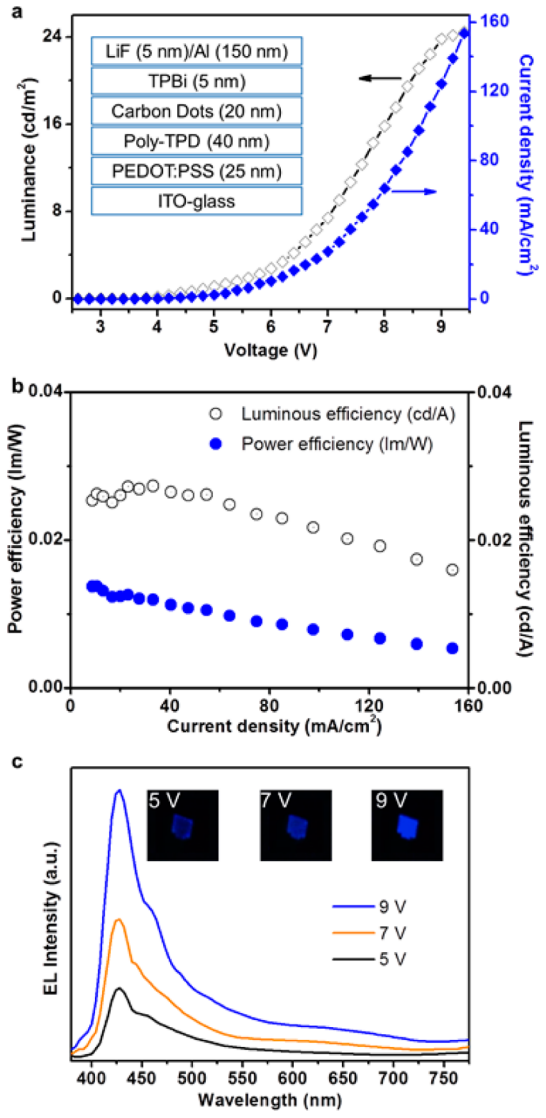

Figure 4. (a) Current density and brightness the CD-LEDs emitting blue light only; the inset shows the LED architecture using a 5 nm LiF layer; (b) the luminous and power efficiency *vs* current density; (c) EL spectra and images of the blue CD-LEDs operated at voltages of 5, 7, and 9 V, respectively.

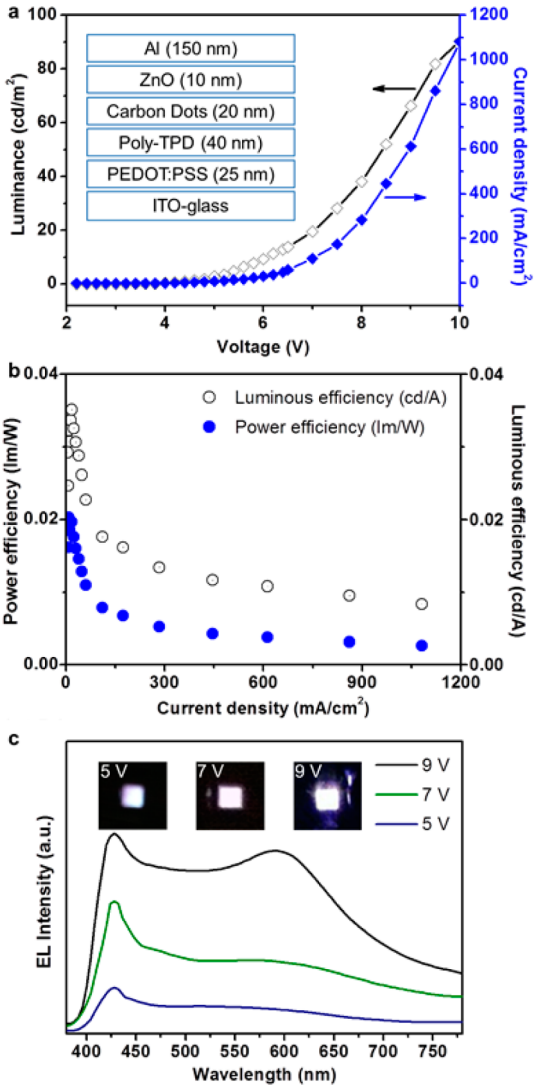

Figure 5. (a) Current density and brightness of the CD-LEDs emitting white light only; the inset shows the white LED architecture using ZnO nanoparticles as an electron transport layer; (b) the luminous and power efficiency *vs* current density; (c) EL spectra of the white emitting CD-LEDs, with true-color photographs of the LEDs operated at different applied voltages.

According to the fluorescence lifetimes of different emission states of the CDs, the steady state PL spectra (Figure 3) indicate that these emissive states are distinct energy levels (centered on 420, 460, and 580 nm), which have their own distinct excitation spectra. In the case of electroluminescence, electrons and holes are injected from the charge injection layers into the emissive layer and only specific type of states will be excited. Since excitation of the specific states in the CDs are distinct (420, 480, and 580 nm) as shown in Figure 3, the excited state that is formed *via* injected charges would emanate from the corresponding emission level associated with each color. The energy state with short lifetime (420 nm) will be very readily depopulated. Therefore, at low current density (or voltage), the carriers will initially be injected into the energy state with short lifetime due to this fast relaxation. When the current density is increased, the more highly populated high energy state can also feed the low energy states (*i.e.*, 480 and 580 nm) and so emission from these levels becomes more significant alongside the direct relaxation from the 420 nm state.

Blue Emitting CD-LED Device. Taking these findings into consideration, the CD-LED device structure was adjusted to control the current density and therefore the EL spectra. One way is to reduce the injection current density by increasing the thickness of the LiF layer to 5 nm (the inset of Figure 4a). Figure 4a shows typical current and luminance curves as a function of the applied voltage for the pure blue emitting CD-LEDs with a cathode of 5-nm LiF and 150-nm aluminum. The devices exhibited low turn-on voltages of 5 V,

confirming a similar minimized barrier for charge injection into the CD-LEDs. The maximum luminance obtained was 24 cd/m^2. The current density was reduced to ~150 mA/cm^2 due to the increased thickness (correspondingly the increased resistance) of the LiF layer (5 nm). The EL spectra of the blue CD-LEDs, operating at different voltages, are shown in Figure 4c; emitting images of the CD-LEDs under operation are also presented in the figure insets. The blue-emitting CD-LED exhibited bright, uniform and defect-free EL emission over the whole bias working range when the current injection was maintained low.

White Emitting CD-LED Device. Low current injection can be used to obtain pure blue emission from the above CD-LEDs. We therefore deduced that high current injection would lead to white emission in the whole working bias. To realize it, we used ZnO nanoparticles as the ETL. The ZnO/CD-LED structure shown schematically in the inset of Figure 5a consisted of layers of ITO/PEDOT:PSS (25 nm, anode), poly-TPD (40 nm, HTL), CDs (20 nm, active emission layer), ZnO nanoparticles (10 nm, ETL), and Al (150 nm, cathode). Figure 5a shows the current-density and luminance changes of the ZnO/CD-LEDs. The maximum luminance for the resulting white light emitting devices reached 90 cd/m^2, which is >2.5 times the reported white light luminance from CD-based LEDs.[44] These ZnO/CD-LEDs exhibited turn-on voltages of 4.6 V, which was lower than those of the TPBI-based devices. The EL spectra measured using a high-sensitivity spectrometer indicated that the light emission from the white CD-LEDs was achieved at a driving voltage as low as 4.6 V, suggesting that electrons and holes could efficiently inject into the CD emitting layer at lower driving voltages. These devices had significantly higher current density than the devices without an ETL, or with a TPBI ETL. As the same HTLs were used in all the CD-LEDs, the high current density was attributed to the more efficient electron injection into the CD layer with a ZnO ETL. This is due to the higher electron mobility of the ZnO nanoparticles which has been reported to be 2×10^{-3} cm^2 V^{-1} s^{-1},[3] at least 1 order of magnitude higher than that of organic ETLs (typically 1×10^{-4} cm^2 V^{-1} s^{-1} or lower).[60,61] With more electrons accumulated at the poly-TPD/CD interface, the interfacial recombination rate is much higher in the ZnO/CD-LEDs than that in the other structures. The white light-emitting CD-LEDs exhibited bright, uniform and defect-free EL emission over the whole bias working range (Figure 5).

CONCLUSIONS

In summary, we have demonstrated solution-processed CD-LEDs based on three different layered structures. Most of the layers in the structures including the conducting polymer hole injection layer, the conjugated polymer hole transport layer, the carbon dot emissive layer, and the organic or ZnO nanoparticle electron transport layer were simply fabricated by spin-coating from solutions; only the anode and cathode layers were vacuum deposited. Depending upon the injection conditions for the respective device structures, the CD-LEDs displayed steady lights (blue or white) or tunable lights (blue, cyan, magenta, and white) from the same 3.3 nm carbon dots. The recorded maximum brightness of the devices was 24 cd/m^2 for blue light and 90 cd/m^2 for white light. Carrier recombination in the CDs was investigated with time-resolved photoluminescence, revealing three luminescence decay processes which were consistent with the EL spectra of the CD-LEDs. Because of the three recombination mechanisms with different decay times, the colorful emission could be obtained and controlled by tuning the injecting current density. Our system shows color variability arising from the presence of three recombination mechanisms in a single CD emitting layer. Therefore, one can envisage creating a multicolor single pixel driven by the current density or voltage. This work will help to develop a better understanding of the recombination mechanisms in CD nanomaterials and to develop promising fabrication techniques for CD-based LEDs applicable for solid state lighting and color displays.

MATERIALS AND METHODS

Carbon Dots Synthesis. The carbon dots employed in the CD-LED devices were synthesized by the approach of Wang *et al.*,[42] using octadecene as the noncoordinating solvent, 1-hexadecylamine as the surface passivation agent, and anhydrous citric acid as the carbon precursor. The CDs were subjected to a multistep precipitation/redisperse process of purification and subsequently dried as solid powders. For microscopic and spectroscopic analyses, powdered CDs were redispersed in toluene.

ZnO Nanoparticle Synthesis. A mixture of 0.44 g zinc acetate and 30 mL ethanol was loaded into a three-neck flask and heated to 75 °C until a clear solution was obtained. After the solution was cooled down to room temperature, 10 mL of NaOH/ethanol solution (0.5 mol/L) was injected into the flask. The solution was stirred for 12 h, and the products were collected by precipitating with hexanes and redispersed in ethanol for device fabrication.

Material Characterization. Transmission electron microscopy (TEM) images of the purified CDs were obtained on a FEI Tecnai F20 microscope operating at 200 keV. Absorption spectra were measured on a Cary 50 absorption spectrometer and PL spectra on a Cary Eclipse spectrofluorimeter. For TRPL measurements, an 800 ps pulsed laser diode with 320 nm wavelength was employed as the excitation source. The TRPL signals were dispersed using a 0.55 m spectrometer and detected using a multichannel plate detector and photomultiplier tubes. The decay traces were recorded using a photon counting method.

Device Fabrication and Characterization. Device fabrication started with a UV-ozone treatment of the ITO-coated substrates to enrich the ITO surface with oxygen and, consequently,

increase the ITO work function.[62] A layer of PEDOT:PSS (~25 nm) was then deposited on the UV-ozone treated ITO surface by spin-coating, followed by annealing in an oven at 120 °C for 10 min in air. Next, the sample was transferred into a nitrogen glovebox system with controlled concentrations of oxygen (≤1 ppm) and water vapor (≤1 ppm), and the poly-TPD HTL, ~40 nm in thickness, was spin-cast on the top of the PEDOT:PSS layer from its chlorobenzene solution and cured at 150 °C for 30 min on a hot plate. Subsequently, the emissive layer of CDs was spin-coated over the surface of poly-TPD HTL from the toluene solution and baked on a hot plate at 80 °C for 30 min to form the active region of the CD-LED. The thickness of the CD-emissive layer was precisely tailored, by varying the CD concentration and the spin speed of the cast deposition, to balance the maximum brightness and emission efficiency of the CD-LEDs. For the TPBI-based device, a ~5 nm thick-TPBI ETL was thermally deposited over the CD-active region, followed by a LiF/Al (1 or 5 nm/150 nm) bilayer cathode which was thermally evaporated through a shadow mask without breaking the vacuum. For the ZnO nanoparticle-based device, a ~10 nm thin ZnO nanoparticle ETL was deposited over the CD-active region by spin coating, and an Al (150 nm) cathode was thermally evaporated through a shadow mask (no LiF layer). The fabricated CD-LEDs had circular shapes, defined by the shadow mask, with a surface area of ~4 mm^2.

The electrical characterization of the devices was performed on a Keithley 2400 source meter. The EL spectra and luminance of the devices (cd/m^2) were measured on a PR650 spectrometer. Images of the LED outputs were recorded with a Sony FWX700 FireWire color CCD camera. All measurements were performed under dark condition.

Conflict of Interest: The authors declare no competing financial interest.

Acknowledgment. This work was financially supported by the National Science Fund for Distinguished Young Scholars (61225018), the National 863 Program (2011AA050509), the National Natural Science Foundation of China (61106039, 51272084), the National Postdoctoral Foundation (2011049015), the Hong Kong Scholar Program (XJ2012022), the Shandong Natural Science Foundation (ZR2012FZ007), the Jilin Talent Fund, the Jilin Province Youth Foundation (201101025), the State Key Laboratory on Integrated Optoelectronics (Jilin University, IOSKL2012ZZ12), and by the Research Grant Council of Hong Kong S.A.R. (project No. T23-713/11).

REFERENCES AND NOTES

1. Anikeeva, P. O.; Halpert, J. E.; Bawendi, M. G.; Bulovic, V. Quantum Dot Light-Emitting Devices with Electroluminescence Tunable over the Entire Visible Spectrum. *Nano Lett.* **2009**, *9*, 2532–2536.
2. Cho, K.-S.; Lee, E. K.; Joo, W.-J.; Jang, E.; Kim, T.-H.; Lee, S. J.; Kwon, S.-J.; Han, J. Y.; Kim, B.-K.; Choi, B. L.; *et al.* High-Performance Crosslinked Colloidal Quantum-Dot Light-Emitting Diodes. *Nat. Photonics* **2009**, *3*, 341–345.
3. Qian, L.; Zheng, Y.; Xue, J.; Holloway, P. H. Stable and Efficient Quantum-Dot Light-Emitting Diodes Based on Solution-Processed Multilayer Structures. *Nat. Photonics* **2011**, *5*, 543–548.
4. Zhang, Y.; Xie, C.; Su, H.; Liu, J.; Pickering, S.; Wang, Y.; Yu, W. W.; Wang, J.; Wang, Y.; Hahm, J.; *et al.* Employing Heavy Metal-Free Colloidal Quantum Dots in Solution-Processed White Light-Emitting Diodes. *Nano Lett.* **2010**, *11*, 329–332.
5. Rogach, A. L.; Lupton, J. Hybrid OLEDs with Semiconductor Nanocrystals. In *Organic Light Emitting Devices*; Mullen, K., Scherf, U., Eds.; Wiley-VCH: Weinheim, Germany, 2006; pp 319−332.
6. Colvin, V.; Schlamp, M.; Alivisatos, A. Light-Emitting Diodes Made from Cadmium Selenide Nanocrystals and a Semiconducting Polymer. *Nature* **1994**, *370*, 354–357.
7. Wood, V.; Bulović, V. Colloidal Quantum Dot Light-Emitting Devices. *Nano Rev.* **2010**, *1*, 5202.
8. Gaponik, N.; Hickey, S. G.; Dorfs, D.; Rogach, A. L.; Eychmüller, A. Progress in the Light Emission of Colloidal Semiconductor Nanocrystals. *Small* **2010**, *6*, 1364–1378.
9. Peng, X. An Essay on Synthetic Chemistry of Colloidal Nanocrystals. *Nano Res.* **2009**, *2*, 425–447.
10. Niu, Y. H.; Munro, A. M.; Cheng, Y.-J.; Tian, Y. Q.; Liu, M. S.; Zhao, J. L.; Bardecker, J. A.; Jen-La Plante, I.; Ginger, D. S.; Jen, A. K.-Y. Improved Performance from Multilayer Quantum Dot Light-Emitting Diodes *via* Thermal Annealing of the Quantum Dot Layer. *Adv. Mater.* **2007**, *19*, 3371–3376.
11. Nizamoglu, S.; Erdem, T.; Sun, X. W.; Demir, H. V. Warm-White Light-Emitting Diodes Integrated with Colloidal Quantum Dots for High Luminous Efficacy and Color Rendering. *Opt. Lett.* **2010**, *35*, 3372–3374.
12. Mutlugun, E.; Hernandez-Martinez, P. L.; Eroglu, C.; Coskun, Y.; Erdem, T.; Sharma, V. K.; Unal, E.; Panda, S. K.; Hickey, S. G.; Gaponik, N.; *et al.* Large-Area (over 50 cm × 50 cm) Freestanding Films of Colloidal InP/ZnS Quantum Dots. *Nano Lett.* **2012**, *12*, 3986–3993.
13. Wu, C. F.; Chiu, D. T. Highly Fluorescent Semiconducting Polymer Dots for Biology and Medicine. *Angew. Chem., Int. Ed.* **2013**, *52*, 3086–3109.
14. Yang, X.; Divayana, Y.; Zhao, D.; Leck, K. S.; Lu, F.; Tan, S. T.; Abiyasa, A. P.; Zhao, Y.; Demir, H. V.; Sun, X. A Bright Cadmium-Free, Hybrid Organic/Quantum Dot White Light-Emitting Diode. *Appl. Phys. Lett.* **2012**, *101*, 233110.
15. Shirasaki, Y.; Supran, G. J.; Bawendi, M. G.; Bulović, V. Emergence of Colloidal Quantum-Dot Light-Emitting Technologies. *Nat. Photonics* **2012**, *7*, 13–23.
16. Sun, Q.; Wang, Y. A.; Li, L.; Wang, D.; Zhu, T.; Xu, J.; Yang, C.; Li, Y. Bright, Multicoloured Light-Emitting Diodes Based on Quantum Dots. *Nat. Photonics* **2007**, *1*, 717–722.
17. Demir, H. V.; Nizamoglu, S.; Erdem, T.; Mutlugun, E.; Gaponik, N.; Eychmüller, A. Quantum Dot Integrated LEDs Using Photonic and Excitonic Color Conversion. *Nano Today* **2011**, *6*, 632–647.
18. Song, W.-S.; Kim, J.-H.; Lee, J.-H.; Lee, H.-S.; Do, Y. R.; Yang, H. Synthesis of Color-Tunable Cu−In−Ga−S Solid Solution Quantum Dots with High Quantum Yields for Application to White Light-Emitting Diodes. *J. Mater. Chem.* **2012**, *22*, 21901–21908.
19. Song, W.-S.; Yang, H. Efficient White-Llight-Emitting Diodes Fabricated from Highly Fluorescent Copper Indium Sulfide Core/Shell Quantum Dots. *Chem. Mater.* **2012**, *24*, 1961–1967.
20. Kim, H. M.; Youn, J. H.; Seo, G. J.; Jang, J. Inverted Quantum-Dot Light-Emitting Diodes with Solution-Processed Aluminium-Zinc Oxide as a Cathode Buffer. *J. Mater. Chem. C* **2013**, *1*, 1567–1573.
21. Rogach, A. L.; Gaponik, N.; Lupton, J. M.; Bertoni, C.; Gallardo, D. E.; Dunn, S.; Li Pira, N.; Paderi, M.; Repetto, P.; Romanov, S. G.; *et al.* Light-Emitting Diodes with Semiconductor Nanocrystals. *Angew. Chem., Int. Ed.* **2008**, *47*, 6538–6549.
22. Kwak, J.; Bae, W. K.; Lee, D.; Park, I.; Lim, J.; Park, M.; Cho, H.; Woo, H.; Yoon, D. Y.; Char, K.; *et al.* Bright and Efficient Full-Color Colloidal Quantum Dot Light-Emitting Diodes Using an Inverted Device Structure. *Nano Lett.* **2012**, *12*, 2362–2366.
23. Chanyawadee, S.; Harley, R. T.; Taylor, D.; Henimi, M.; Susha, A. S.; Rogach, A. L.; Lagoudakis, P. G. Efficient Light Harvesting in Hybrid CdTe Nanocrystal/Bulk GaAs p-i-n Photovoltaic Devices. *Appl. Phys. Lett.* **2009**, *94*, 233502.
24. Hu, W.; Henderson, R.; Zhang, Y.; You, G.; Wei, L.; Bai, Y.; Wang, J.; Xu, J. Near-Infrared Quantum Dot Light Emitting Diodes Employing Electron Transport Nanocrystals in a Layered Architecture. *Nanotechnology* **2012**, *23*, 375202.
25. Keuleyan, S.; Lhuillier, E.; Guyot-Sionnest, P. Synthesis of Colloidal HgTe Quantum Dots for Narrow Mid-IR Emission and Detection. *J. Am. Chem. Soc.* **2011**, *133*, 16422–16424.
26. Rogach, A.; Harrison, M. T.; Kershaw, S. V.; Kornowski, A.; Burt, M. G.; Eychmüller, A.; Weller, H. Colloidally Prepared CdHgTe and HgTe Quantum Dots with Strong Near-Infrared Luminescence. *Phys. Status Solidi B* **2001**, *224*, 153–158.

27. Steckel, J. S.; Coe-Sullivan, S.; Bulović, V.; Bawendi, M. G. 1.3 to 1.55 μm Tunable Electroluminescence from PbSe Quantum Dots Embedded within an Organic Device. *Adv. Mater.* **2003**, *15*, 1862–1866.
28. Sun, L.; Choi, J. J.; Stachnik, D.; Bartnik, A. C.; Hyun, B.-R.; Malliaras, G. G.; Hanrath, T.; Wise, F. W. Bright Infrared Quantum-Dot Light-Emitting Diodes Through Inter-Dot Spacing Control. *Nat. Nanotechnol.* **2012**, *7*, 369–373.
29. Konstantatos, G.; Huang, C.; Levina, L.; Lu, Z.; Sargent, E. H. Efficient Infrared Electroluminescent Devices Using Solution-Processed Colloidal Quantum Dots. *Adv. Funct. Mater.* **2005**, *15*, 1865–1869.
30. Chung, W.; Jung, H.; Lee, C. H.; Park, S. H.; Kim, J.; Kim, S. H. Synthesis and Application of Non-toxic $ZnCuInS_2$/ZnS Nanocrystals for White LED by Hybridization with Conjugated Polymer. *J. Electrochem. Soc.* **2011**, *158*, H1218–H1220.
31. Chung, W.; Jung, H.; Lee, C. H.; Kim, S. H. Fabrication of High Color Rendering Index White LED Using Cd-Free Wavelength Tunable Zn Doped $CuInS_2$ Nanocrystals. *Opt. Express* **2012**, *20*, 25071–25076.
32. Sun, Y.-P.; Zhou, B.; Lin, Y.; Wang, W.; Shiral Fernado, K. A.; Pathak, P.; Meziani, M. J.; Harruff, B. A.; Wang, X.; Wang, H.; *et al.* Quantum-Sized Carbon Dots for Bright and Colorful Photoluminescence. *J. Am. Chem. Soc.* **2006**, *128*, 7756–7757.
33. Baker, S. N.; Baker, G. A. Luminescent Carbon Nanodots: Emergent Nanolights. *Angew. Chem., Int. Ed.* **2010**, *49*, 6726–6744.
34. Wang, F.; Xie, Z.; Zhang, H.; Liu, C. Y.; Zhang, Y. G. Highly Luminescent Organosilane-Functionalized Carbon Dots. *Adv. Funct. Mater.* **2011**, *21*, 1027–1031.
35. Cao, L.; Wang, X.; Meziani, M. J.; Lu, F.; Wang, H.; Luo, P. G.; Lin, Y.; Harruff, B. A.; Veca, L. M.; Murray, D.; *et al.* Carbon Dots for Multiphoton Bioimaging. *J. Am. Chem. Soc.* **2007**, *129*, 11318–11319.
36. Wang, X.; Cao, L.; Yang, S.-T.; Lu, F.; Meziani, M. J.; Tian, L.; Sun, K. W.; Bloodgood, M. A.; Sun, Y. P. Bandgap-Like Strong Fluorescence in Functionalized Carbon Nanoparticles. *Angew. Chem., Int. Ed.* **2010**, *49*, 5310–5314.
37. Zhu, S.; Meng, Q.; Wang, L.; Zhang, J.; Song, Y.; Jin, H.; Zhang, K.; Sun, H.; Wang, H.; Yang, B. Highly Photoluminescent Carbon Dots for Multicolor Patterning, Sensors, and Bioimaging. *Angew. Chem., Int. Ed.* **2013**, *52*, 3953–3957.
38. Zhang, H.; Huang, H.; Ming, H.; Li, H.; Zhang, L.; Liu, Y.; Kang, Z. Carbon Quantum Dots/Ag_3PO_4 Complex Photocatalysts with Enhanced Photocatalytic Activity and Stability under Visible Light. *J. Mater. Chem.* **2012**, *22*, 10501–10506.
39. Cao, L.; Sahu, S.; Anilkumar, P.; Bunker, C. E.; Xu, J.; Shiral Fernando, K. A.; Wang, P.; Guliants, E. A.; Tackett, K. N.; Sun, Y. P. Carbon Nanoparticles as Visible-Light Photocatalysts for Efficient CO_2 Conversion and Beyond. *J. Am. Chem. Soc.* **2011**, *133*, 4754–4757.
40. Wang, X.; Cao, L.; Lu, F.; Meziani, M. J.; Li, H.; Qi, G.; Zhou, B.; Harruff, B. A.; Kermarrec, F.; Sun, Y. P. Photoinduced Electron Transfers with Carbon Dots. *Chem. Commun.* **2009**, *25*, 3774–3776.
41. Guo, X.; Wang, C.-F.; Yu, Z.-Y.; Chen, L.; Chen, S. Facile Access to Versatile Fluorescent Carbon Dots toward Light-Emitting Diodes. *Chem. Commun.* **2012**, *48*, 2692–2694.
42. Wang, F.; Pang, S.; Wang, L.; Li, Q.; Kreiter, M.; Liu, C.-Y. One-Step Synthesis of Highly Luminescent Carbon Dots in Noncoordinating Solvents. *Chem. Mater.* **2010**, *22*, 4528–4530.
43. Photopoulos, P.; Nassiopoulou, A. G. Room- and Low-Temperature Voltage Tunable Electroluminescence from a Single Layer of Silicon Quantum Dots in between Two Thin SiO_2 Layers. *Appl. Phys. Lett.* **2000**, *77*, 1816–1818.
44. Xuan, R.-W; Xu, J.-P.; Zhang, X.-S.; Li, P.; Luo, C.-Y.; Wu, Y.-Y.; Li, L. Continuously Voltage-Tunable Electroluminescence from a Monolayer of ZnS Quantum Dots. *Appl. Phys. Lett.* **2011**, *98*, 041907.
45. Xiao, B.; Wu, X. L.; Xu, W.; Chu, P. K. Tunable Electroluminescence from Polymer-Passivated 3C-SiC Quantum Dot Thin Film. *Appl. Phys. Lett.* **2012**, *101*, 123110.
46. Wang, F.; Chen, Y.-H.; Liu, C.-Y.; Ma, D.-G. White Light-Emitting Devices Based on Carbon Dots' Electroluminescence. *Chem. Commun.* **2011**, *47*, 3502–3504.
47. Carter, J. C.; Grizzi, I.; Heeks, S. K.; Lacey, D. J.; Latham, S. G.; May, P. G.; Ruiz de los Paños, O.; Pichler, K.; Towns, C. R.; Wittmann, H. F. Operating Stability of Light-Emitting Polymer Diodes Based on Poly(*p*-phenylene vinylene). *Appl. Phys. Lett.* **1997**, *71*, 34–36.
48. Sun, Q. J.; Fan, B. H.; Tan, Z. A.; Yang, C. H.; Li, Y. F.; Yang, Y. White Light from Polymer Light-Emitting Diodes: Utilization of Fluorenone Defects and Exciplex. *Appl. Phys. Lett.* **2006**, *88*, 163510.
49. Sun, Q. J.; Hou, J. H.; Yang, C. H.; Li, Y. F.; Yang, Y. Enhanced Performance of White Polymer Light-Emitting Diodes Using Polymer Blends as Hole-Transporting Layers. *Appl. Phys. Lett.* **2006**, *89*, 153501.
50. Li, H.; Kang, Z.; Liu, Y.; Lee, S.-T. Carbon Nanodots: Synthesis, Properties and Applications. *J. Mater. Chem.* **2012**, *22*, 24230–24253.
51. Li, X.; Wang, H.; Shimizu, Y.; Pyatenko, A.; Kawaguchi, K.; Koshizaki, N. Preparation of Carbon Quantum Dots with Tunable Photoluminescence by Rapid Laser Passivation in Ordinary Organic Solvents. *Chem. Commun.* **2010**, *47*, 932–934.
52. Tian, L.; Ghosh, D.; Chen, W.; Pradhan, S.; Chang, X.; Chen, S. Nanosized Carbon Particles from Natural Gas Soot. *Chem. Mater.* **2009**, *21*, 2803–2809.
53. Luo, Z.; Lu, Y.; Somers, L. A.; Johnson, A. C. High Yield Preparation of Macroscopic Graphene Oxide Membranes. *J. Am. Chem. Soc.* **2009**, *131*, 898–899.
54. Tetsuka, H.; Asaho, R.; Nagoya, A.; Okamoto, K.; Tajima, I.; Ohta, R.; Okamoto, A. Optically Tunable Amino-Functionalized Graphene Quantum Dots. *Adv. Mater.* **2012**, *24*, 5333–5338.
55. Yu, P.; Wen, X. M.; Toh, Y. R.; Tang, J. Temperature-Dependent Fluorescence in Carbon Dots. *J. Phys. Chem. C* **2012**, *116*, 25552–25557.
56. Dong, Y.; Pang, H.; Yang, H.; Guo, C.; Shao, J.; Chi, Y.; Li, C.; Yu, T. Carbon-Based Dots Co-doped with Nitrogen and Sulfur for High Quantum Yield and Excitation-Independent Emission. *Angew. Chem., Int. Ed.* **2013**, *52*, 7800–7804.
57. Wang, L.; Zhu, S.; Wang, H.; Wang, Y.; Hao, Y.; Zhang, J.; Chen, Q.; Zhang, Y.; Han, W.; Yang, B.; *et al.* Unraveling Bright Molecule-Like State and Dark Intrinsic State in Green-Fluorescence Graphene Quantum Dots *via* Ultrafast Spectroscopy. *Adv. Optical Mater* **2013**, *1*, 264–271.
58. Kapitonov, A. M.; Stupak, A. P.; Gaponenko, S. V.; Petrov, E. P.; Rogach, A. L.; Eychmuller, A. Luminescence Properties of Thiol-Stabilized CdTe Nanocrystals. *J. Phys. Chem. B* **1999**, *103*, 10109–10113.
59. Lunz, M.; Gerard, V. A.; Gun'ko, Y. K.; Lesnyak, V.; Gaponik, N.; Susha, A. S.; Rogach, A. L.; Bradley, A. L. Surface Plasmon Enhanced Energy Transfer Between Donor and Acceptor CdTe Nanocrystal Quantum Dot Monolayers. *Nano Lett.* **2011**, *11*, 3341–3345.
60. Forrest, S. R. The Path to Ubiquitous and Low-Cost Organic Electronic Appliances on Plastic. *Nature* **2004**, *428*, 911–918.
61. Eom, S.-H.; Zheng, Y.; Wrzesniewski, E.; Lee, J.; Chopra, N.; So, F.; Xue, J. Effect of Electron Injection and Transport Materials on Efficiency of Deep-Blue Phosphorescent Organic Light-Emitting Devices. *Org. Electron.* **2009**, *10*, 686–691.
62. Kim, J.; Friend, R.; Cacialli, F. Surface Energy and Polarity of Treated Indium−Tin−Oxide Anodes for Polymer Light-Emitting Diodes Studied by Contact-Angle Measurements. *J. Appl. Phys.* **1999**, *86*, 2774–2778.